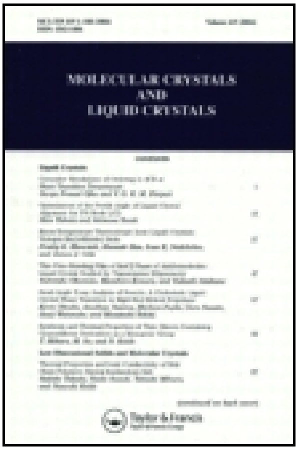

Molecular Crystals and Liquid Crystals
Publication details, including instructions for authors and subscription information:
http://www.tandfonline.com/loi/gmcl20

Design of Polysiloxane Materials for Electronic Applications

Yusuke Kawakami [a], Yeong Hee Cho [a], Man He [a] & Lei Xue [a]

[a] School of Materials Science, Japan Advanced Institute of Science and Technology (JAIST), Ishikawa, Japan

Version of record first published: 23 Aug 2006

To cite this article: Yusuke Kawakami, Yeong Hee Cho, Man He & Lei Xue (2006): Design of Polysiloxane Materials for Electronic Applications, Molecular Crystals and Liquid Crystals, 447:1, 189/[507]-202/[520]

To link to this article: http://dx.doi.org/10.1080/15421400500387502

Mol. Cryst. Liq. Cryst., Vol. 447, pp. 189/[507]–202/[520], 2006
Copyright © Taylor & Francis Group, LLC
ISSN: 1542-1406 print/1563-5287 online
DOI: 10.1080/15421400500387502

Design of Polysiloxane Materials for Electronic Applications

Yusuke Kawakami
Yeong Hee Cho
Man He
Lei Xue
School of Materials Science, Japan Advanced Institute of Science and Technology (JAIST), Ishikawa, Japan

Dehydrocoupling reaction catalyzed by palladium was used to synthesize aromatic-substituted poly(carbosiloxane)s having potentiality to be used as thermo-resistant insulating materials. Well-defined transmission holographic gratings with high diffraction efficiency were fabricated by the introduction of siloxane components: 1) to mesogenic compounds, 2) to bifunctional epoxides as cationically polymerizable monomers, which polymerize slower than radically polymerizable multi-functional acrylate.

Keywords: bis(epoxide); electrical insulator; holographic grating; multi-functional acrylate; siloxane

INTRODUCTION

Modern advanced technologies have continuous demands on the development of long-term stable functional materials. As elastomers for electronic applications, thermal stability up to two hundred degree is required simultaneously maintaining flexibility to temperatures much lower than ambience. Polysiloxanes are good candidates for such functional materials because of flexible and heat resistant Si–O–Si

This work was partly supported by a Grant-in-Aid for Scientific Research (16205016) from the Ministry of Education, Science, Sports, Culture and Technology, Japan. This work was also carried out partly in the Nanotechnology Glass Project, as part of the Nanotechnology Materials Program supported by the New Energy and Industrial Technology Development Organization (NEDO).

Address correspondence to Yusuke Kawakami, School of Materials Science, Japan Advanced Institute of Science and Technology (JAIST), 1-1 Asahidai, Nomi, Ishikawa, 923-1292, Japan. E-mail: kawakami@jaist.ac.jp

backbone, which is also the origin of good dielectric and surface properties [1,2], and silarylene-siloxane polymers, derivatives of polysiloxanes by partially replacing –O– by arylene groups, show better mechanical property than polysiloxane [3,4].

Merker reported polycondensation of bis(1,4-dimethylsilylbenzene) (BHSB) to give poly[(oxydimethylsilylene)(1,4-phenylene)(dimethylsilylene)] [5], commonly called as poly(tetramethyl-*p*-silphenylenesiloxane) (PTMPS). This PTMPS contains the maximum number of rigid phenylene groups, and should be reluctant to siloxane rearrangement and highly thermally stable. We reported a clean method to obtain PTMPS by catalytic cross-dehydrocoupling polymerization of 1,4-bis(dimethylsilyl)benzene with water under neutral condition [6]. However, PTMPS is crystalline, and proper chemical modification of the structure should be made in some applications. A kind of poly(silphenylenesiloxane)s containing hydride and vinyl side groups, which have been proved to be promising candidates for high temperature elastomers [7]. Vinyl side functions can also be chemically cured or modified by various reactions such as hydrosilylation to give new functionality or a 3-D network structure to the polymer. The cross-linking density may also be controlled over a broad range depending on the ratio of the cross-linker to vinyl groups.

Meanwhile, photopolymers are very useful and attractive materials for many applications, such as information storage media [8–10] and photonic devices [11,12], and even as photo-curable coating materials [13,14]. Optical holography [15–18] promises storage densities and data-transfer rates which far exceed those of traditional magnetic and optical recording technologies. Success in further development of holograms for various applications depends on the creation of hologram gratings with high resolution and sharp angle selectivity by considering the characteristics of the materials.

Multi-functional acrylate systems, such as DuPont's HRF [19,20] series and Polaroid's DMP-128 [21], have been most widely developed for holography recording. These materials provide high performance and permanently fixed holograms, although they have some drawbacks such as volume shrinkage and multi-step processing.

R. L. Sutherland [22–25] created the switchable holograms for photonic applications by combining the liquid crystals with multifunctional acrylate systems, and explored the electro-optical effects by considering their large dielectric anisotropy and optical birefringence. Diffraction efficiency close to 100% was obtained, and the Bragg gratings showed a very narrow angular selectivity ($<1^\circ$). Kawabata [26] developed a novel photopolymer systems consisting of a radically polymerizable monomer (RPM) and a cationically polymerizable monomer (CPM) to write reflection holograms.

Recently, we have focused on the study of siloxane-containing compounds as holographic recording materials by taking advantage of the characteristic chemical and physical properties of siloxane chain. Siloxane component was expected to induce clear phase separation between bright and dark regions of light interference and large modulation of refractive index, due to their incompatibility and difference in refractive index compared with carbon-based matrix materials, and flexibility to ease fast diffusion.

RESULTS AND DISCUSSION

The synthetic scheme of poly(silphenylenesiloxane) is illustrated in Scheme 1.

As an example of the modification of chemical structure of poly(silphenylenesiloxane), analysis of the polymers was carried out for the polymers obtained from isomeric bis(dimethylsilyl)benzene. From size exclusion chromatographic analysis of the product mixture before purification, it was found that the low molecular weight fraction increased with the increase of *m*-dimethylsilylbenzene in the feed. The oligomer fraction was proved to be essentially the cyclic dimer by NMR and MS spectra. Melting point was observed at 127°C for the polymer from *p*-isomer. There were no melting points for the polymers containing *m*-isomer. The crystallinity of polymer from *p*-isomer could be controlled by the incorporation of small amounts of *m*-isomer in the polymer structure.

Poly(silphenylenesiloxane) with molecular weight range 3,000 to 10,000 has a good possibility to be applied as high performance insulating resin in semi-conductor chip production. Catalytic cross-dehydrocoupling polymerization reactions of 1,5-dihydro-1,5-dimethyl-3,3,7,7-tetraphenylcyclotetrasiloxane with water and diols gave polymers with cyclosiloxane moiety.

In the formation of holographic gratings using photo cross-linkable system with trimethylolpropane triacrylate (TMPTA) and

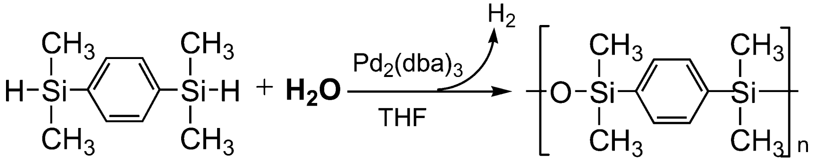

SCHEME 1 Synthetic Scheme of Poly(silphenylenesiloxane).

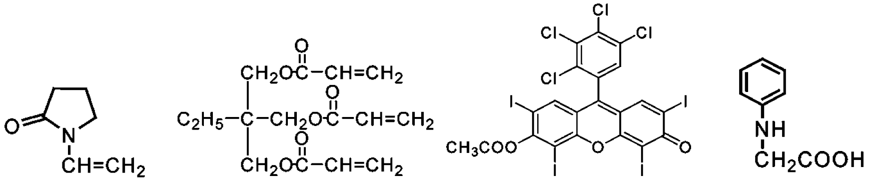

NVP TMPTA Rose Bengal *N*-Phenylglycine

FIGURE 1 Structures of radically polymerizable reactive diluent, trifunctional monomer, and photoinitiating system.

N-vinylpyrrolidinone (NVP) system, (siloxane and mesogen)-containing compounds were effective over a wide concentration range from 3 wt% to 30 wt%. Structures of radically polymerizable monomers and initiator system are shown in Figure 1.

Structure of (siloxane and mesogen)-containing compounds are shown in Figure 2.

Diffraction efficiency is one of very important factor to evaluate the grating performance. The diffraction efficiency is defined as the ratio of diffraction intensity (I_d) to sum of transmitted beam intensities ($I_d + I_t$) after recording, as illustrated in Figure 3.

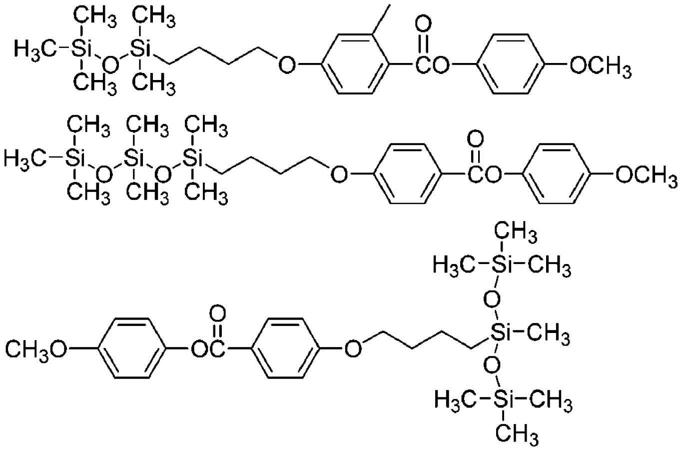

A MW 446.7

B MW 520.8

C MW 520.8

FIGURE 2 Chemical structures of (siloxane and mesogen)-containing compounds. **A**: 1-(4′-methoxyphenyloxycarbonylphenoxy)butyl-1,1,3,3,3-pentamethyldisiloxane, **B**: 1-(4′-methoxyphenyloxycarbonylphenoxy)butyl-1,1,3,3,5,5,5-heptamethyltrisiloxane, **C**: 3-(4′-methoxyphenyloxycarbonylphenoxy)-butyl-1,1,1,3,5,5,5-heptamethyltrisiloxane.

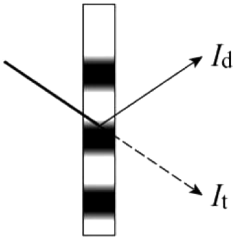

$$\eta\ (\%) = \frac{I_d}{I_d + I_t} \times 100$$

FIGURE 3 Definition of diffraction efficiency.

A fine and improved grating with 40% diffraction efficiency was formed with 10 wt% compound **A** by changing the concentration of NVP as shown in Figure 4. The real-time diffraction efficiencies are shown in Figure 5. Under low NVP concentration (<45 wt%), the diffraction efficiency was typically <13%. It was assumed that high cross-linking density (NVP < 45 wt% in mixture) decreases phase separation by shortening the gelation time of the multi-functional monomer, thus, though the elastic driving force is strong, most **A** was retained in the polymer matrix, hence, the efficiency was reduced. Sharp increases of

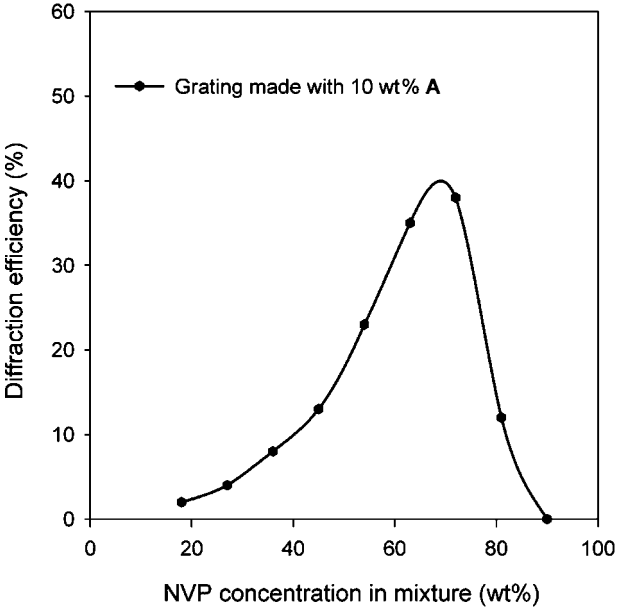

FIGURE 4 Diffraction efficiency of the grating made with **A**.

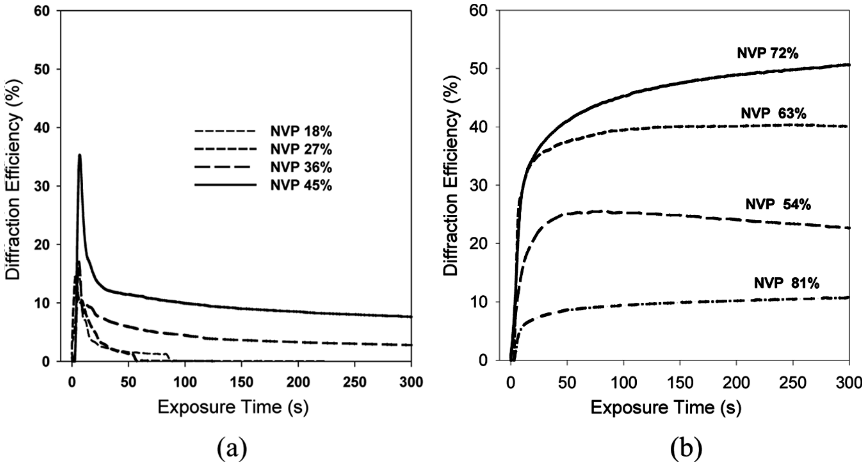

FIGURE 5 Real-time diffraction efficiency of grating made with **A** and at (a) low and (b) high NVP concentration.

diffraction efficiency in the initial stage of the exposure time indicated the fast polymerization and cross-linking of the TMPTA.

When NVP concentration is increased to 72 wt% (Fig. 5(b)), the diffraction efficiency reached 38% and slightly increased to over 50% with prolonged curing time. This result suggests that increasing NVP concentration will enhance the phase separation by increasing the diffusion rate of **A**. The slight increase of diffraction efficiency might cause by the slow photo-reaction of NVP, or by the diffusion of **A** from the gelated polymer.

The resulting grating was examined to study the nature of the grating film and its optical performance by AFM and SEM. 3-D morphology and depth profile of the original grating sample fabricated from 90 wt% matrix (TMPTA:NVP = 4:6) and 10 wt% **A**, and its washed sample with ethanol are shown in Figure 6.

A clear grating morphology of a periodic interference fringe pattern can be observed both in Figure 6(a) and (b). The evenly stratified composite film with periodic alternating layers is attributable to the effective phase separation of **A** from polymer matrix. The hilltop region in Figure 6(a) is considered as the polymer region covered with some **A**. This flat and shallow morphology strongly suggests that after the gelation of the polymer, a part of the remaining **A** diffused out from the polymer matrix region and attached to the polymer surface, due to the mobility of **A** and its chemical incompatibility with the polymer. Spacing of grating is observed as 0.96 μm and 0.93 μm before and after

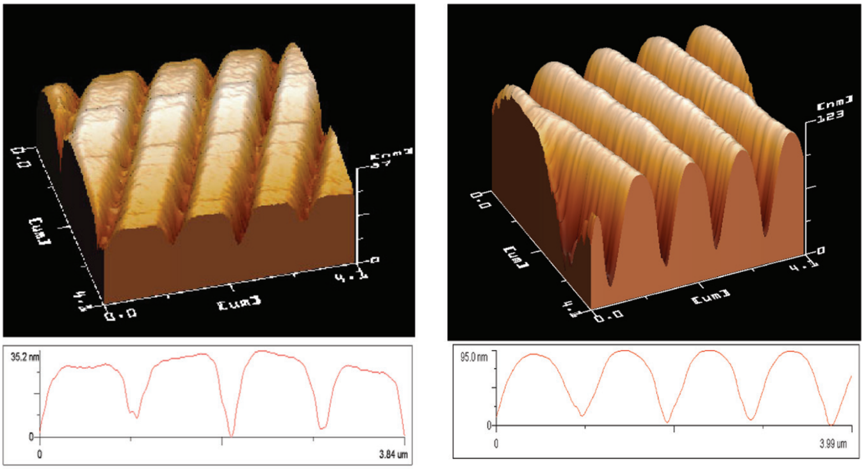

(a) (b)

FIGURE 6 AFM morphology and surface profile of the grating obtained with **A** (a) as produced, and (b) after washing with ethanol.

removal of the **A**, and the depth of grating is much deeper (99 nm) after washing than that before washing (35 nm). Such morphology seemed to be correlated to the high diffraction efficiency.

SEM observation clearly showed the formation of discrete grating as shown in Figure 7. Angular selectivity of grating with **A** is shown in Figure 8. Narrow angular selectivity is very important for the optical performance of grating like high density image storage.

In the formation of gratings by photopolymer system, difference in polymerization rate is one of the important factors to obtain

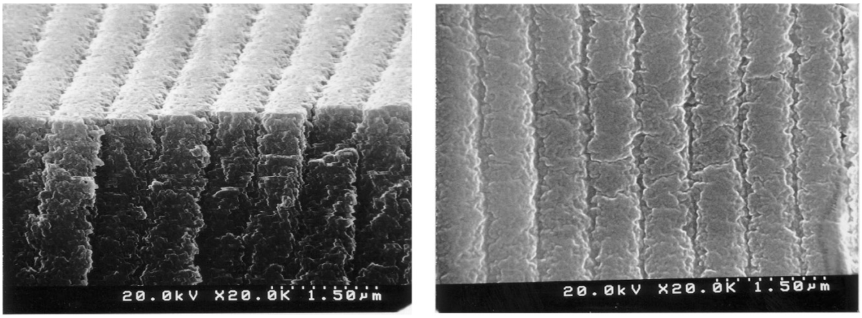

(a) (b)

FIGURE 7 Edge (a) and top (b) view of the grating observed by SEM.

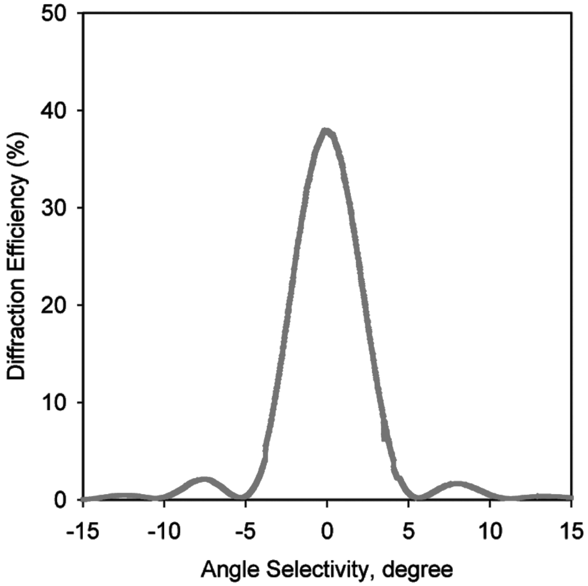

FIGURE 8 Angular selectivity of grating prepared with **A**.

fine grating. Typical chemical structure of vinyl monomers (RPM) and cationically ring-opening polymerizable monomers (CPM) to be used in photopolymer system are shown in Figures 9 and 10.

For simple nonslanted transmission gratings, maximum diffraction efficiency is given by Kogelnik's coupled wave theory [27]:

$$\eta = \sin^2[\pi \Delta \mathrm{n}\, T/\lambda]$$

where η is the maximum diffraction efficiency, Δn is the modulation of refractive index of the recording medium after recording, T is the thickness of the hologram, and λ is the recording wavelength.

In this research, T and λ were fixed as 20 µm and 532 nm, respectively. Thus diffraction efficiency was mainly affected by Δn which can

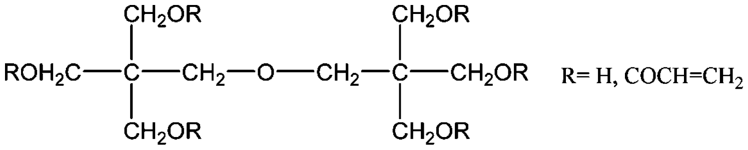

$$\mathrm{ROH_2C{-}C(CH_2OR)_2{-}CH_2{-}O{-}CH_2{-}C(CH_2OR)_2{-}CH_2OR}$$

R= H, $COCH{=}CH_2$

Dipentaerythritol penta-/hexa-acrylate

FIGURE 9 Chemical structures of multi-functional acrylate (MFA) as RPM.

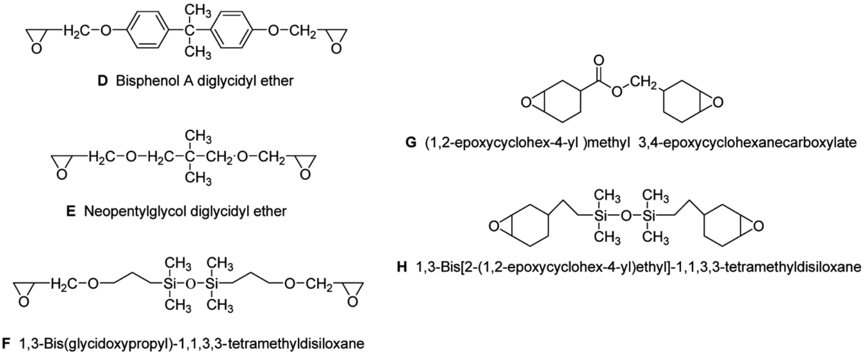

FIGURE 10 Chemical structures of ring-opening polymerizable epoxides as CPM.

be varied by chemical structure of recording materials. When the contrast of refractive index of CPM and RPM materials is large, Δn value becomes larger if their phase separation is perfect, thus η value also becomes large.

Roughly estimated refractive index and diffraction efficiency of the formed gratings, and modulation of refractive index for all the CPMs are summarized in Table 1.

Diffraction efficiency for glycidyl ether derivatives increased in the order of **D** < **E** < **F**, although contrast of refractive index was **E** < **F** < **D**. Among cyclohexene oxide derivatives, **G** showed the lowest efficiency. These orders are not completely in accordance with the order of the contrast of refractive index. In the present photopolymerizable system, Δn, which plays important role to determine the diffraction efficiency, depends not only on the static contrast of refractive index between MFA and CPM, but also on the dynamic phase separation process. If the reaction rate of a CPM is too fast, some CPMs are left in the high intensity fringes, and precise modulation will not be generated. The effects of intensity of irradiation beams are shown in Figure 11.

TABLE 1 Refractive Index, Viscosity, Modulation of Refractive Index, and Diffraction Efficiency of the Grating Made with Compounds D, E and F

Structure	Refractive index	Viscosity	Modulation of refractive index(Δn)	Diffraction efficiency (%)
D	1.586	3450	0.00517	34
E	1.457	31	0.00751	62
F	1.452	9	0.00922	80

In radical photopolymerization systems, polymerization rate (R_p) is proportional to the illumination intensity [28];

$$R_p = (\Phi I_0)^{\delta}(k_p/2k_t^{1/2})[\mathrm{M}]$$

In which, Φ is the overall initiation efficiency of the process, I_0 is the illumination intensity, and δ is the value determined by reaction environments. The coefficients k_p and k_t are the rate constants of chain propagation and termination, respectively, and [M] is the concentration of monomer.

According to Kogelnik's coupled wave theory, diffraction efficiency should be changed as a sinusoidal mode by modulation of refractive index caused by polymerization. As typically shown in Figure 11, in case of **F**, the diffraction efficiency reached to over 90% at the intensity of 10 mW/cm^2. Decrease in the intensity to 5 mW/cm^2 decreased the efficiency to about 81%. It may be understood that under very low intensity of 5 mW/cm^2, polymerization rate of MFA itself became slow, and poorly cross-linked polymer matrix could not repel F toward low intensity fringes, and resulted in only lower diffraction efficiency. These changes were roughly sinusoidal.

Figure 12 shows the AFM of holographic gratings formed with cyclohexene oxide derivatives as CPM.

Figure 13 shows the surface profiles of gratings made with **G** and **H**. Grating made with **H** having very smooth surface, showed the highest

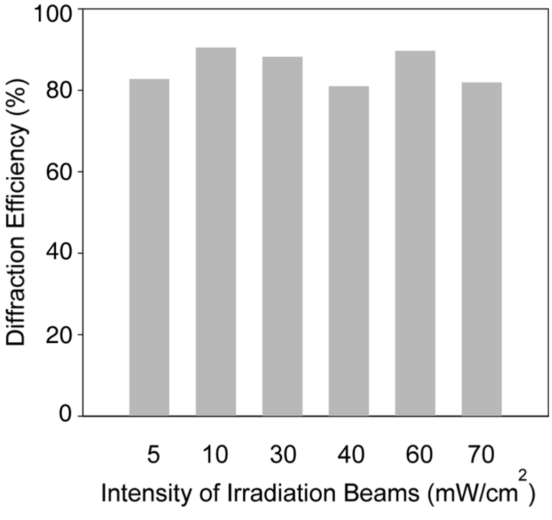

FIGURE 11 Effects of intensity of irradiation beams on diffraction efficiency of holographic gratings formed with structure F.

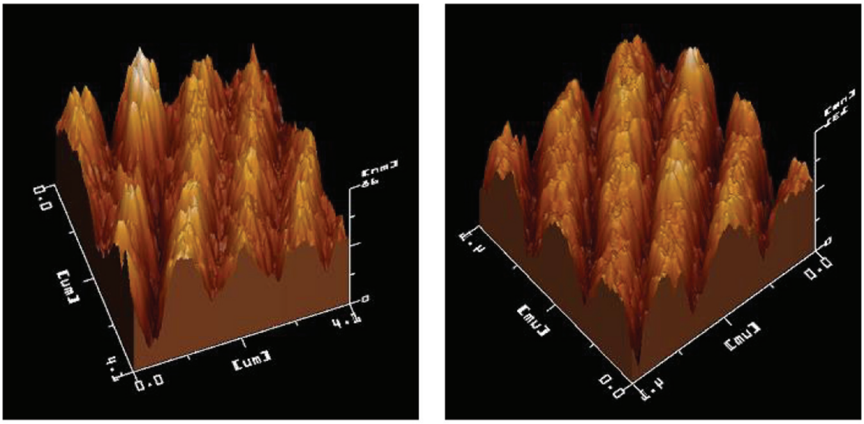

(a) (b)

FIGURE 12 AFM of transmission holographic gratings formed with cyclohexene derivatives as CPM; (a) **G**, and (b) **H**.

grating depths (about 86 nm). That with **G** has shallow grating depths (about 55 nm), and rough and irregular surface profiles, which is in accordance with the order of diffraction efficiency. Further study should be done in order to optimize the polymerization rate and diffusion rate by varying the ratio of RPM and CPM.

To further study the effects of siloxane-containing derivatives on morphologies of gratings, SEM measurement was carried out.

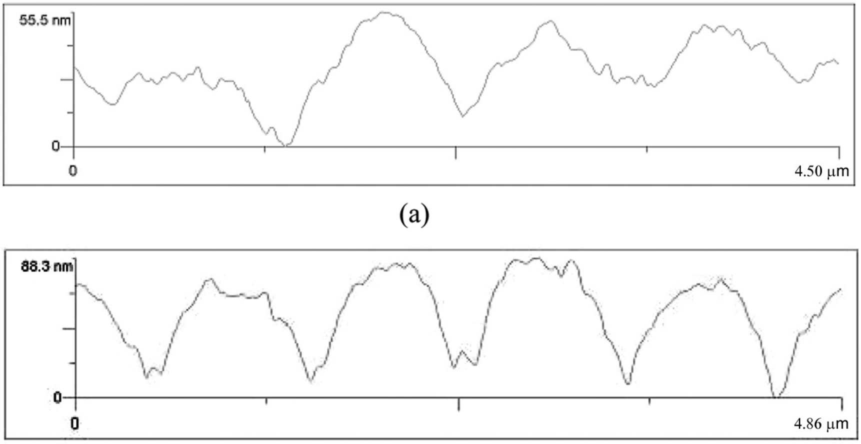

(a)

(b)

FIGURE 13 Surface profiles of the gratings prepared with **G** and **H**.

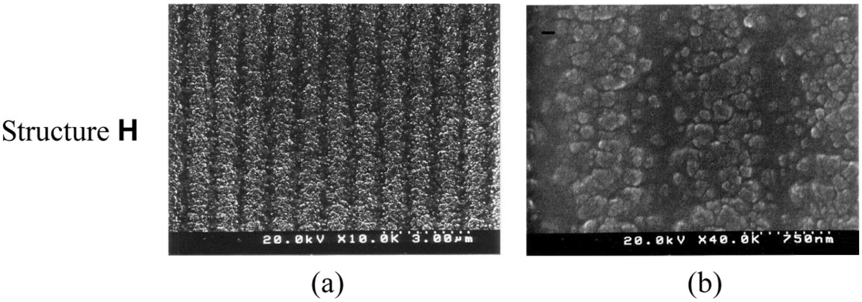

FIGURE 14 SEM morphologies of the grating fabricated with **H**; (a) low magnification: × 10.0 K and (b) high magnification: × 40.0 K.

Figure 14 shows the SEM of gratings made with **H** as CPM. Bright and dark regions are polymer layers formed from RPM and CPM, respectively. Although good phase separation between polymer layers formed from RPM and CPM was observed for all compounds, **F** especially gave well-controlled phase separated structure.

As typically shown in Figure 15, angular selectivity widths were similar for all samples with different structures of epoxides (about 3°).

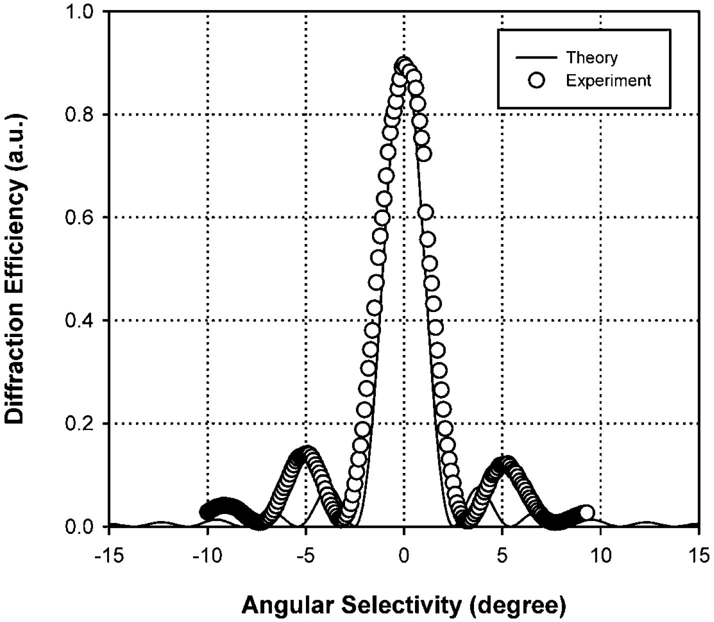

FIGURE 15 Angular selectivity for holographic gratings prepared with **F**.

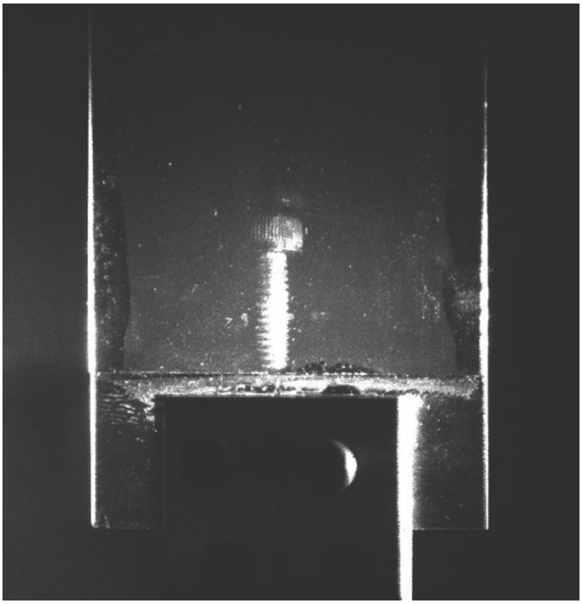

FIGURE 16 The real image of a screw recorded in the grating prepared with **H**.

This value is in a good agreement with calculated value by the Kogelnik's coupled wave theory. Adjustment of sample thickness and inter-beam angle is needed to further reduce the angular selectivity.

Real-images of a screw were successfully stored by CCD camera in gratings made with various epoxide-containing systems. The image stored in the grating with **H**, which showed clear and stable phase-separated structure, as CPM is shown in Figure 16.

CONCLUSION

We have demonstrated a new catalytic reaction to give polymers with siloxane linkage. Poly(arylenesiloxane)s are good candidate to be used for materials as advanced insulating materials. Gratings of high diffraction efficiency were prepared by the introduction of siloxane component into mesogen-containing compounds. Fine holographic gratings were prepared via different reaction and diffusion rates using epoxides as CPM. Especially, siloxane-containing CPM induced good diffusion and phase separation during the formation of holographic gratings. Well-fabricated gratings with high diffraction efficiency and angle selectivity of $<3^\circ$ were created, and real-image of a screw was successfully stored.

REFERENCES

[1] Dvornic, P. R. & Lenz, R. W. (Eds.) (1990). *High Temperature Siloxane Elastomers*, Hüthig & Wepf: Basel.

[2] Zeigler, J. M. & Fearon, G. F. W. (Eds.) (1990). *Silicon-Based Polymer Science: A Comprehensive Resource*, American Chemical Society: Washington, DC.

[3] Breed, L. W., Elliott, R. L., & Whitehead, M. E. (1967). *J. Polym. Sci., Part A-1*, *5*, 2745.

[4] Burks, R. E., Covington, E. R., Jackson, M. V., & Curry, J. E. (1973). *J. Polym. Sci. Polym. Chem. Ed.*, *11*, 319.

[5] Merker, R. L. & Scott, M. J. (1964). *J. Polym. Sci., Part A: Polym. Chem.*, *2*, 15.

[6] (a) Li, Y. & Kawakami, Y. (1999). *Macromolecules*, *32*, 3540.
(b) Li, Y. & Kawakami, Y. (1999). *Macromolecules*, *32*, 6871.
(c) Li, Y. & Kawakami, Y. (1999). *Macromolecules*, *32*, 8768.

[7] Liu, Y., Imae, I., Makishima, A., & Kawakami, Y. (2003). *Science and Technology of Advanced Materials*, *4*, 27.

[8] Trentler, T. J., Boyd, J. E., & Colvin, V. L. (2000). *Chem. Mater.*, *12*(5), 1431.

[9] Bunning, T. J., Kirkpatrick, S. M., Natarajan, L. V., Tondiglia, V. P., & Tomlin, D. W. (2000). *Chem. Mater.*, *12*(10), 2842.

[10] Joo, W. J., Oh, C. H., Song, S. H., Kim, P. S., & Han, Y. K. (2001). *J. Phys. Chem. B*, *105*(35), 8322.

[11] Yoneyama, S., Yamamoto, T., Tsutsumi, O., Kanazawa, A., Shiono, T., & Ikeda, T. (2002). *Macromolecules*, *35*(23), 8751.

[12] Berkovic, G., Krongauz, V., & Weiss, V. (2000). *Chem. Rev.*, *100*(5), 1741.

[13] Tomlinson, W. J., Chandross, E. A., Weber, H. P., & Aumiller, G. D. (1976). *Applied Optics*, *15*(2), 534.

[14] Hsieh, M. D. & Zellers, E. T. (2002). *Sensors and Actuators B*, *82*, 287.

[15] Heanue, J. F., Bashaw, M. C., & Hesselink, L. (1994). *Science*, *265*, 749.

[16] Psaltis, D. (2002). *Science*, *298*, 1359.

[17] Shen, X. A., Nguyen, A., Perry, J. W., Huestis, D. L., & Kachru, R. (1997). *Science*, *278*, 96.

[18] Coufal, H. (1998). *Nature*, *393*, 628.

[19] Weber, A. M., Smothers, W. K., Trout, T. J., & Mickish, D. J. (1990). *Proc. SPIE-Int. Soc. Opt. Eng.*, *1212*, 30.

[20] Gambogi, W. J., Weber, A. M., & Trout, T. J. (1993). *Proc. of SPIE-holographic Imaging and Materials*, *2043*, 2.

[21] Ingwall, R. T. & Fielding, H. L. (1985). *Opt. Eng.*, *24*, 808.

[22] Bunning, T. J., Natarajan, L. V., Tondiglia, V. P., & Sutherland, R. L. (2000). *Annu. Rev. Mater. Sci.*, *30*, 83.

[23] Natarajan, L. V., Shepherd, C. K., Brandelik, D. M., Sutherland, R. L., Chandra, S., Tondiglia, V. P., Tomlin, D., & Bunning, T. J. (2003). *Chem. Mater.*, *15*(12), 2477.

[24] Pogue, R. T., Sutherland, R. L., Schmitt, M. G., Natarajan, L. V., Siwecki, S. A., Tondiglia, V. P., & Bunning, T. J. (2000). *Applied Spectroscopy*, *54*(1), 12A.

[25] Sutherland, R. L., Natarajan, L. V., Tondiglia, V. P., & Bunning, T. J. (1993). *Chem. Mater.*, *5*, 1533.

[26] Kawabata, M., Sato, A., Sumiyoshi, I., & Kubota, T. (1993). *Proc. SPIE*, *66*, 1914.

[27] Kogelnik, H. (1969). *Bell Syst. Tech. J.*, *48*, 2909.

[28] Mishra, M. K. & Yagci, Y. (1998). *Handbook of Radical Vinyl Polymerization*, Marcel Dekker, Inc.: New York.